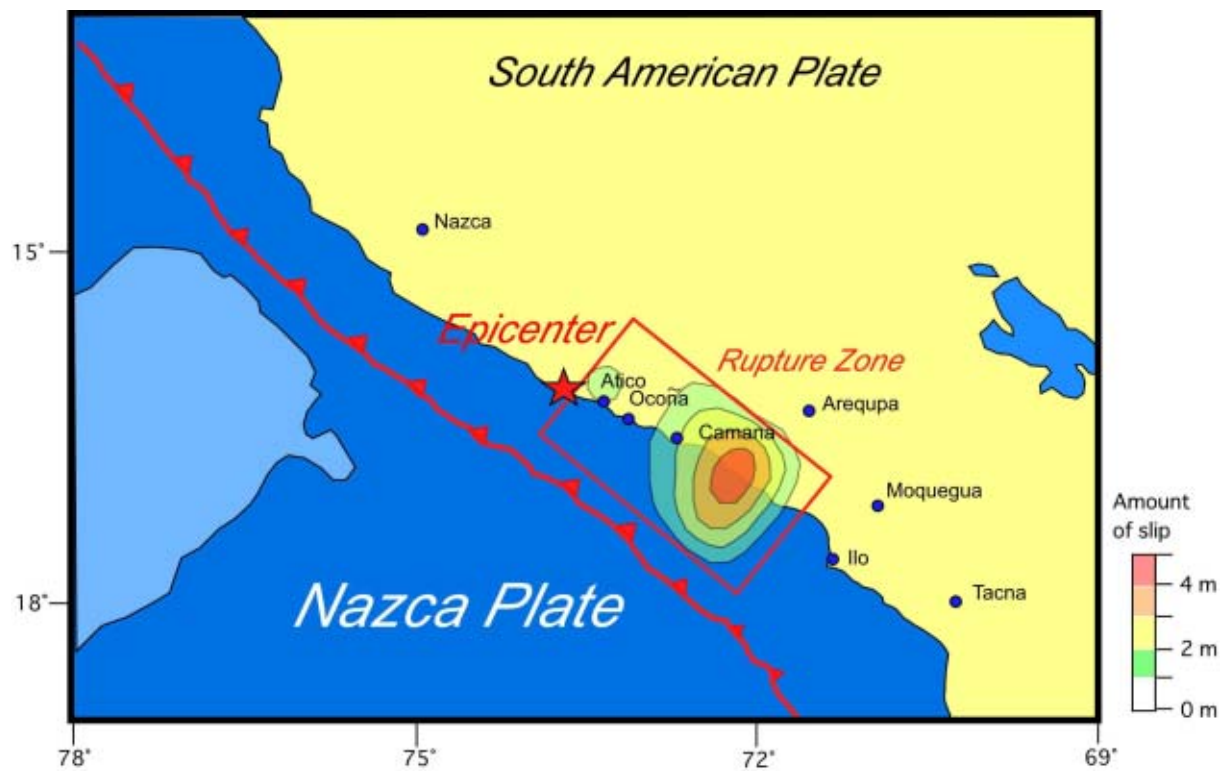


## 2. SEISMICITY, STRONG GROUND MOTIONS AND GEOLOGY

### 2.1 SOURCE CHARACTERISTICS

Atico Earthquake occurred off the coast of southern Peru, about 175 km west of Arequipa or about 595 km southeast of Lima at 4:33 PM EDT on Jun 23, 2001 (3:33 PM local time in Peru). A revised moment magnitude of 8.4 (Harvard) was computed for this earthquake, making this the largest earthquake to occur anywhere in the world in the past 25 years. The focal depth was shallow, with estimates from 9 km (Sipkin, USGS), 26 km (Harvard) to 40 km (Univ of Tokyo). This earthquake was produced by the subduction of the Nazca plate beneath the South American plate. The final slip distribution of the main event, from the inversion of teleseismic body-waves (Kikuchi and Yamanaka, 2001) shows a 300-km zone striking northwest extending from Chala to south of Motegua with two asperities: a large asperity is located at the southeast side of the zone and a smaller asperity located in the northwest end of the zone (**Figure 2.1**). Source parameters obtained by the analysis of teleseismic body-waves are shown in **Table 2.1**. The rupture surface inferred from the distribution of aftershocks (**Figure 2.2**) agrees well with the estimated fault model.



**Figure 2.1** Source Inversion of the teleseismic body-waves (IRIS-DMC) of the June 23, 2001 Atico Earthquake (Kikuchi and Yamanaka, 2001). The location of epicenter is after Tavera et al (2001).

**Table 2.1** Fault parameters of the main shock (after Kikuchi and Yamanaka, 2001)

Epicenter	16.14°S, 73.31°W
Strike, Dip angle, Rake	309, 21, 61
Seismic moment	$2.2 \times 10^{21}$ Nm (Mw=8.2)
Process time	107 sec.
Depth	30 km
Fault area	200×100 km <sup>2</sup>
Dislocation	Dmax=4.5 m Dmean=Mo/ $\mu$ S=2.8 m ( $\mu$ =40GPa)
Stress drop	$\Delta\sigma = 2.5 \text{ Mo/S}^{1.5} = 1.9 \text{ Mpa}$

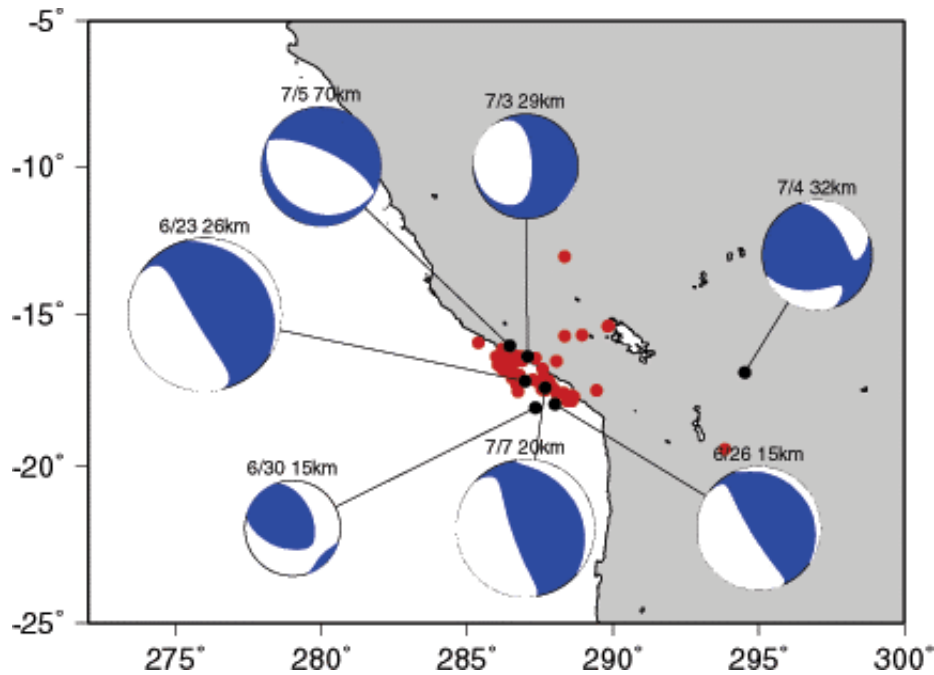


**Figure 2.2** Distribution of aftershocks and their focal mechanisms and depth (after Kikuchi and Yamanaka, 2001). The information of aftershocks are based on USGS (23 June – 29 June, 2001) and focal mechanisms are after Harvard CMT solutions.

The geometry of the upper surface of the subducting Nazca plate is well documented by many authors, using the distribution of hypocenters (Barazangi and Isacks, 1979; Hasegawa and Sacks, 1981; Tavera and Bufo, 1998; Bernal, 2000). The **Figure 2.3** shows the hypocentral distribution map of the southern part of Peru and **Figure 2.4** represents the estimated profiles of the upper surface of the Nazca plate based on the hypocentral distribution after Bernal (2000). **Figure 2.5** shows the 3D geometry of the upper surface of the Nazca plate. The dip angle of slab along the southern most part of the Peruvian coast (15°S to 18°S) is steeper than that along the northern part. The hypocenter of the Atico earthquake is located near the southern flank of the subducting Nazca Ridge and the rupture zone is located on the slab which showing relatively steeper angle than in the northern part.

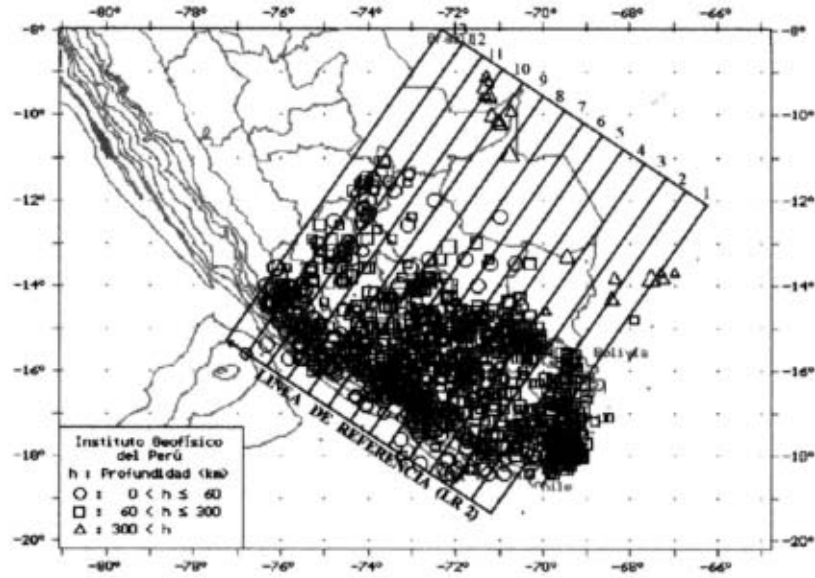


**Figure 2.3** Seismicity of the southern part of Peru during 1970-1995 (after Bernal, 2000). The hypocenters ( $mb \geq 4$ ) are plotted. Numbers suggest the location of profiles shown in Figure 2.3.

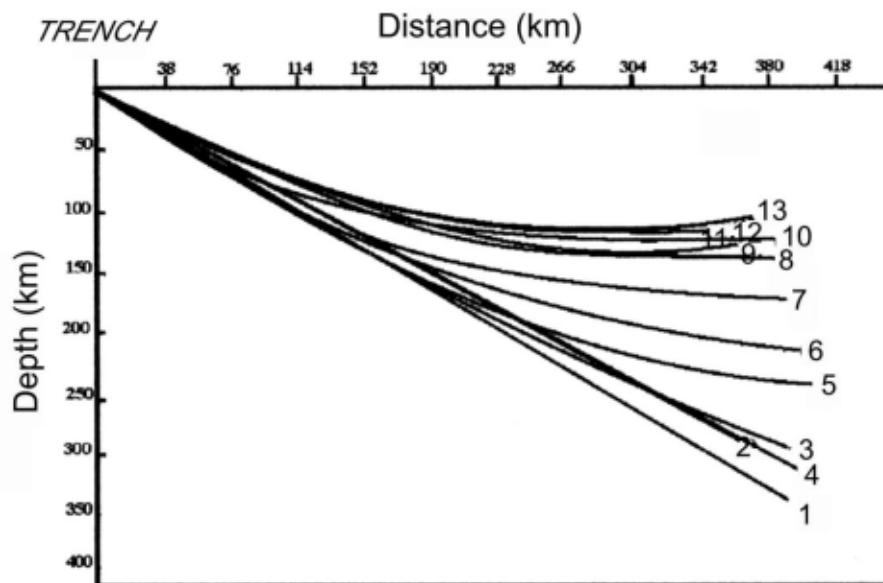


**Figure 2.4** Profiles of the upper surface of Nazca plate in the southern part of Peru (after Bernal, 2000). The locations of profiles are shown in **Figure 2.3**

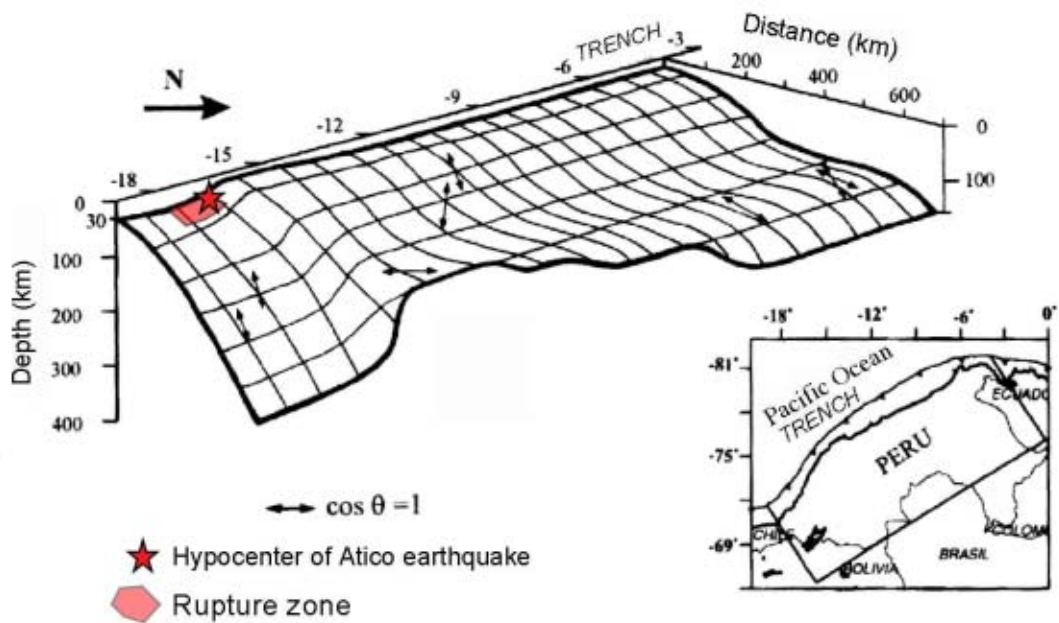


**Figure 2.5** Schematic diagram showing the geometry of upper surface of the Nazca plate (Tavera and Buforn, 1998) and the rupture zone of Atico earthquake. Arrows indicate the direction of tensional stress axis.

Since the 1994 Bolivian deep-focus earthquake ( $M_w$  8.2; Kirby et al., 1995), the southern Peruvian coast and the northern Chile coast experienced three large subduction earthquakes, such as the 1995 Antofagasta earthquake ( $M_w$  8.0; Delouis et al., 1997), the 1996 Nazca Ridge earthquake ( $M_w$  8.0; Spence et al., 1999) and the 2001 Atico earthquake. The rupture areas by these earthquakes are shown in **Figure 2.6**. The hypocenter of the Atico earthquake is located just south of the rupture area of the 1996 Nazca Ridge earthquake. The large portion of the rupture area of the Atico earthquake overlaps with that of the 1868 earthquake ( $M_w$  8.8-9.1; Comte and Pardo, 1991). The area between the rupture areas of the 2001 Atico earthquake and 1995 Antofagasta earthquake still remains un-ruptured. According to Dorbath et al. (1990), southern Peruvian coast ( $16^\circ\text{S}$  to  $18^\circ\text{S}$ ) has experienced three great earthquakes ( $M_w > 8$ ) since 1600 AD; they include the 1604 ( $M_w$  8.7), 1784 ( $M_w$  8.4) and 1868 ( $M_w$  8.8) earthquakes. After Comte and Pardo (1991), the return period for the zone of 1868 earthquake is estimated to be  $118 \pm 33$  years and  $111 \pm 33$  years for the zone of 1877 earthquake. Since the 1994 Bolivian deep-focus earthquake is directly downdip from the Atico earthquake, the sequential occurrence of large earthquakes in southern Peru and northern Chile since 1994 seems to be closely related. Thus, the seismic risk in the area between the rupture zones of the 2001 Atico earthquake and 1995 Antofagasta earthquake is estimated to be very high.

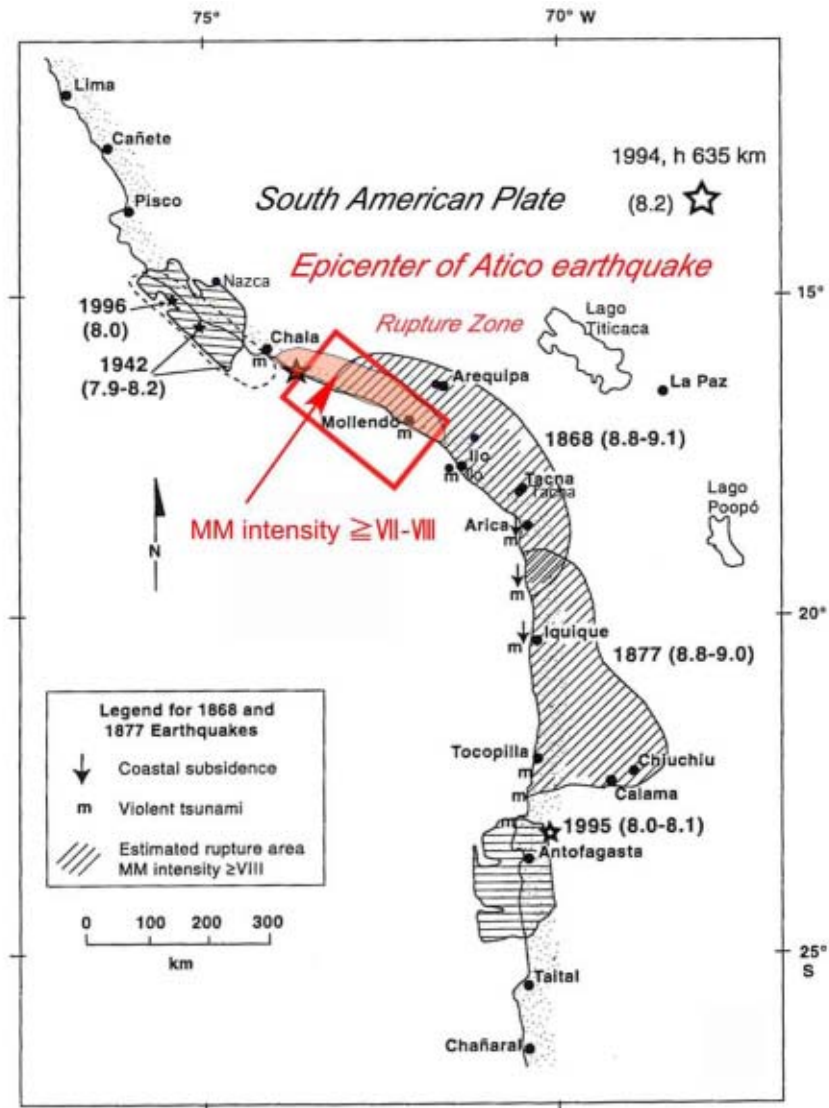


**Figure 2.6** The distribution of rupture zones of large earthquakes in the southern Peru after Spence et al. (1999). The location of epicenter and intensity of Atico earthquake is after Tavera et al. (2001).

## 2.2 GROUND MOTION CHARACTERISTICS

CISMID (Japan-Peru Center for Earthquake Engineering and Disaster Mitigation) has recovered and processed the information from only one instrument that triggered in Peru, the one in the city of Moquegua. Two other instruments in the epicentral area apparently malfunctioned. **Figures 2.7** and **8** show the corrected ground acceleration time histories and the corresponding acceleration response spectra obtained from that instrument recording in East-West, North-South, and Vertical directions.

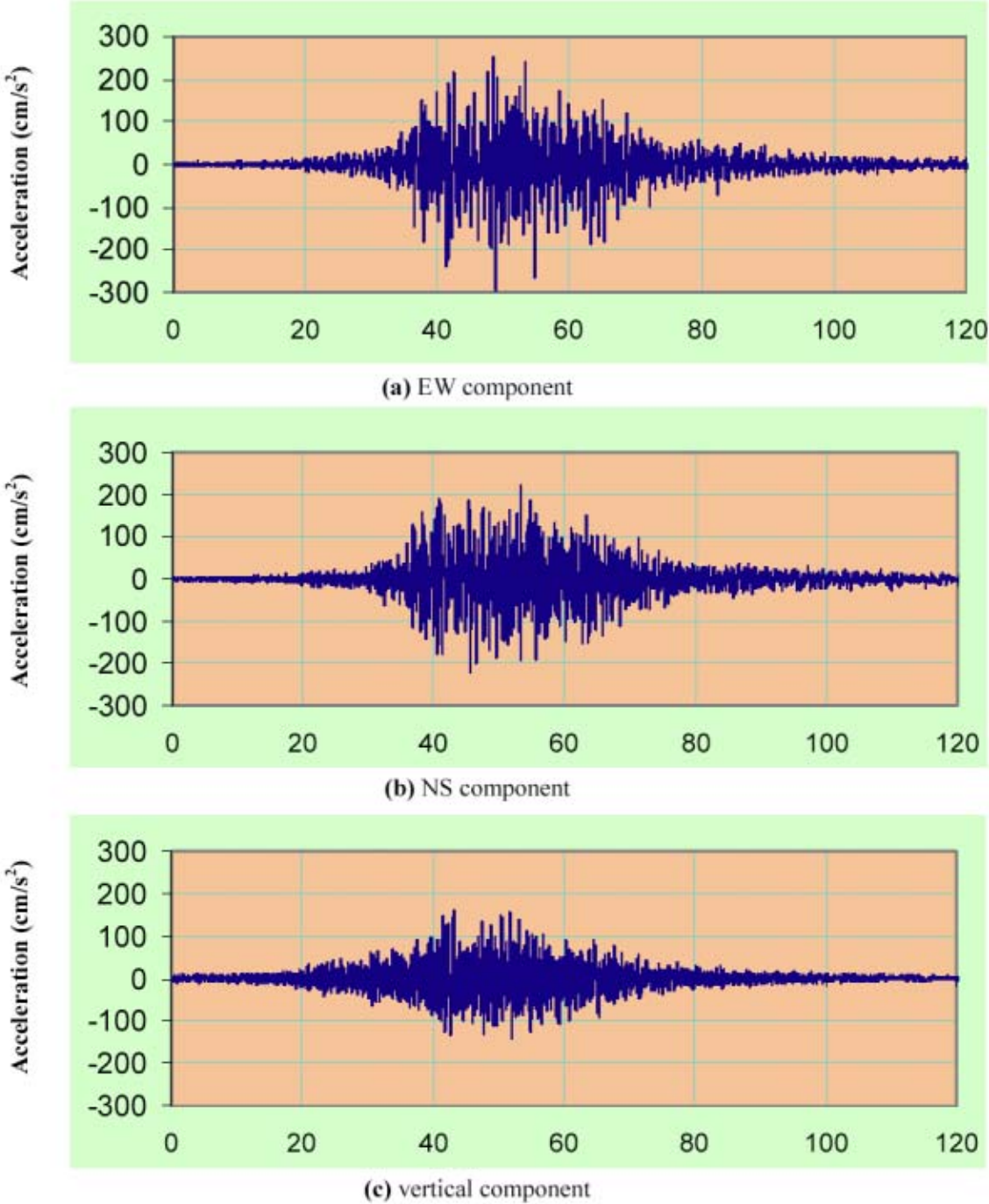
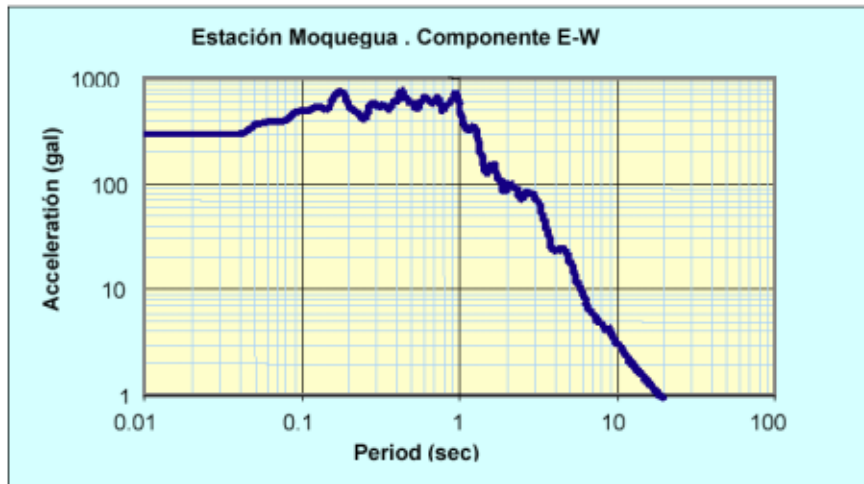
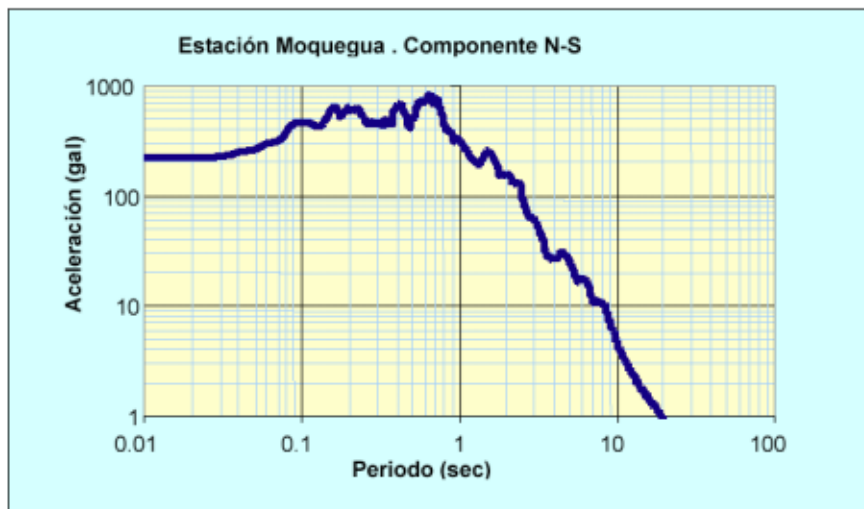


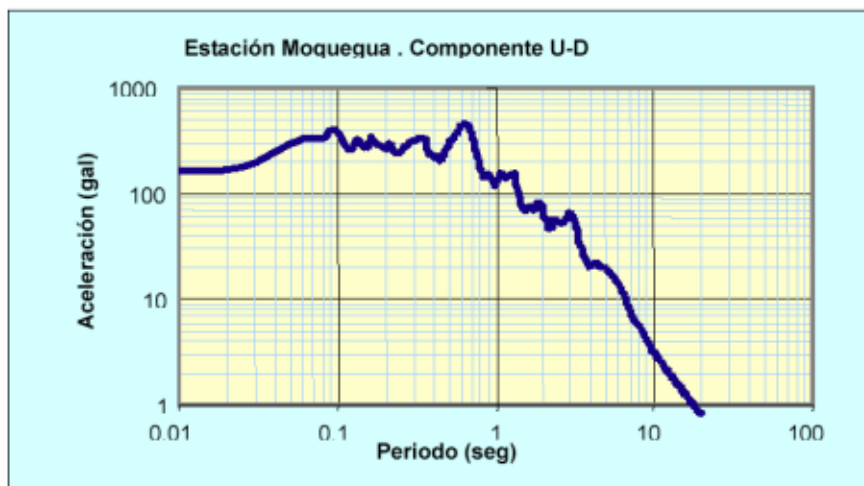
**Figure 2.7** Acceleration time histories at Moquegua



(a) EW component



(b) NS component



(c) UD component

Figure 2.8 Acceleration time histories at Moquegua

 [to the next page](#)